Research Article

Received: 23 July 2017 Revised: 21 September 2017 Accepted article published: 28 September 2017 Published online in Wiley Online Library: 30 November 2017

(wileyonlinelibrary.com) DOI 10.1002/jctb.5455

In situ purification of periplasmatic L-asparaginase by aqueous two phase systems with ionic liquids (ILs) as adjuvants

João HPM Santos,[a,b] Juan C Flores-Santos,[b] Giovanna P Meneguetti,[b] Carlota O Rangel-Yagui,[b] João AP Coutinho,[a] Michele Vitolo,[b] Sónia PM Ventura[a*] and Adalberto Pessoa Jr[b]

Abstract

BACKGROUND: L-asparaginase (ASNase) is an important biopharmaceutical used to treat the acute lymphoblastic leukemia (ALL) and lymphosarcoma. Considering its main use in cancer therapy, the most important request for ASNase production is the need for a highly pure biopharmaceutical obtained in the final of the downstream process, which is considered as the crucial step in its production.

RESULTS: This work proposes the use of polymer–salt aqueous two-phase systems (ATPS) based on polyethylene glycol and citrate buffer, with ionic liquids (ILs) as adjuvants, combined with the permeabilization of cell membrane using n-dodecane and glycine for the *in situ* purification of periplasmatic ASNase from *Escherichia coli* cells. The process proposed was optimized (polymer molecular weight, pH, tie-line length/mixture point, presence, nature and concentration of the adjuvant). The results show that ASNase partitions mostly to the PEG-rich phase, due to hydrophobic interactions between both PEG and enzyme. Remarkably, the addition of 5 wt% of 1-butyl-3-methylimidazolium methanesulfonate [C_4mim][CH_3SO_3] as adjuvant lead to high recoveries [87.94 ± 0.03 (%)], purification factors (20.09 ± 0.35), and a final specific activity SA = 3.61 ± 0.38 U mg^{-1} protein, from a crude enzyme extract with a SA = 0.18 ± 0.05 U mg^{-1} protein. Moreover, better results were achieved when a prepurification step consisting of an ammonium sulfate precipitation was combined with the optimized ATPS, achieving an increased SA = 22.01 ± 1.36 U mg^{-1} protein and PF = 173.8.

CONCLUSIONS: A novel integrated downstream process was successfully implemented for the *in situ* purification of ASNase from fermentation broth.

Keywords: therapeutic enzyme; L-asparaginase; aqueous two-phase systems; ionic liquids as adjuvants; integrated *in situ* purification process

INTRODUCTION

L-asparaginase, L-asparagine amidohydrolase, EC.3.5.1.1 (ASNase) is a biopharmaceutical produced mostly by *Escherichia coli*[1,2] that has been widely studied as a therapeutic agent in the treatment of specific tumour types, including acute lymphoblastic leukemia (ALL)[3–5] in humans and canine lymphosarcoma.[6,7] ASNase was approved for medical use in the United States in 1978[8] and, since then it is on the World Health Organization's List of Essential Medicines.[9] The underlying principle behind the ASNase anti-cancer mechanism of action is deprivation of the essential amino acid L-asparagine for leukemic cells, which require exogenous sources of this amino acid for their survival.[10] ASNase catalyses the conversion of L-asparagine to aspartic acid and ammonia.[2] Its commercial manufacture conventionally uses downstream processes such as unit chemical lysis,[11] protein precipitation,[12–15] centrifugation,[16] filtration,[13,17] fluidised bed chromatography,[11] and other chromatographic techniques[12,15,16,18–20] (e.g. ion-exchange, gel filtration and immobilized metal affinity chromatography - IMAC). Recently, new strategies were developed regarding the purification of ASNase, namely those based in aqueous two-phase extraction (ATPE) via aqueous two-phase systems (ATPS) and aqueous micellar two-phase systems (AMTPS).[17,21] The *in situ* ATPE strategies are combining different cell disruption approaches with the use of ATPS, resulting in higher product yields and lower costs associated to the enzyme purification. Moreover, it can also increase the productivity of the downstream process[22–26] by the elimination of antagonists (including proteases or other product-degrading agents). Actually, through the differential partition behaviour of

* *Correspondence to: SPM Ventura, Campus Universitário de Santiago, 3810-193, Aveiro, Portugal. Email: spventura@ua.pt*

a *CICECO - Aveiro Institute of Materials, Department of Chemistry, University of Aveiro, Portugal*

b *School of Pharmaceutical Sciences, University of São Paulo, São Paulo, Brazil*

the target product and antagonists, or the so-called contaminants also present in the bulk after the cell disruption, the product hydrolysis/denaturation is also reduced.[17,27] Furthermore, the industrial scale-up in continuous flow of these integrated processes based in the combination of efficient cell disruption and ATPS is simpler and faster and more productive than the batch operations.[17,26,28]

In this ambit, the first AMTPS described for ASNase purification was composed of Triton X-100 and potassium phosphate (K_2HPO_4).[21] However, this system leads to enzyme inactivation by antagonists (e.g. proteases and carbohydrases), high ionic strength, and protein interactions with cell debris, resulting in product loss. Moreover, one of the major drawbacks of AMTPS is the difficulty to remove the surfactant (approximately 15 w/v%) from the enzyme solution. In the same line, Zhu *et al.*[17] proposed ATPS and AMTPS composed of phosphate buffer (KH_2PO_4/K_2HPO_4) and polyethylene glycol (PEG) or poloxamers (poly(propylene glycol) block with poly(ethylene glycol), PEG-PPG-PEG). The purification factors obtained with these systems were quite low, from 0.75–3.37, probably due to the high salting-out ability of phosphate salts resulting in the proteins (target and contaminants) preferential partition to the polymer-rich phase. Moreover, this work was mainly focused on the application of AMTPS, the PEG/salt-based ATPS being poorly optimized. Conditions, like PEG molecular weight (MW), tie-line length (TLL), pH and mixture point, normally resulting in big effects were completely neglected in this work. In addition, the phosphate buffer has great interference with the methods of ASNase quantification (Nessler[29] and aspartate hydroxamate[30] assays) used in this work, which is another factor explaining the lower values of purification obtained. Due to the low purification data obtained and the higher purity required to apply ASNase as a biopharmaceutical, it would be important to develop novel and more efficient *in situ* downstream integrated processes.

Ionic liquids (ILs) are salts in which the ions are poorly coordinated, which results in these compounds being liquid below 100 °C.[31] Moreover, these liquid salts exhibit tunable physicochemical properties related to their *designer solvent* character, through the manipulation of a large range of cations and anions. Most ILs are soluble in water and have been used as phase forming compounds in ATPS.[32] Recently, ILs have been applied as additives in the ATPS formation, as adjuvants[33–35] and electrolytes[36,37] in polymer-based ATPS, showing outstanding results in the purification of biomolecules. In this way, the presence of ILs in small amounts was proved to potentiate significantly the purification performance of ATPS, when compared with systems with no adjuvant.[33–35]

In this work, novel polymer–salt ATPS based on polyethylene glycol (PEG) and the biodegradable and nontoxic organic salt citrate buffer with ILs as adjuvants for the *in situ* purification of periplasmatic ASNase from *Escherichia coli*, were investigated. The conditions, polymer molecular weight, pH, TLL/mixture point, presence and nature of adjuvant and its concentration, were extensively investigated to optimize the ATPS purification performance. For the most promising *in situ* ATPS, an additional step of pre-purification consisting of enzyme precipitation with ammonium sulfate was applied in order to further enhance the productivity and purification of ASNase. The integrated process of purification and isolation of ASNase will be proposed.

METHODS AND MATERIALS

Chemicals

The polyethylene oxide polymers, PEG 2000, 4000, 6000, 8000, as well as the potassium citrate, citric acid and ammonium sulphate (> 95 wt%) were purchased from Sigma-Aldrich (St. Louis, MO, USA). The ILs used in this work as adjuvants were 1-butyl-3-methylimidazolium chloride ($[C_4mim]Cl$), 1-butyl-3-methylimidazolium dimethyl phosphate ($[C_4mim][DMP]$), 1-butyl-3-methylimidazolium methanesulfonate ($[C_4mim][CH_3SO_3]$) and 1-butyl-3-methylimidazolium triflate $[C_4mim][CF_3SO_3]$. The ILs were purchased from Iolitec (Heilbronn, Deutschland), with purity >97 wt%. The water content of ILs was measured and taken into account in the preparation of the ATPS. Ultrapure water by reverse-osmosis (Millipore Co. Ltd.) was used in all experiments. All chemicals used in the upstream process of ASNase, and protein and activity assays were purchased from Sigma-Aldrich (St. Louis, MO, USA).

Preparation of crude enzyme extract

Escherichia coli BL21 (DE3) (Novagen, WI, USA) harbouring vector (pET15b + ansB) and ampicillin resistance gene as selection marker was grown on Luria Bertani (LB) agar plate containing: tryptone (10 g L^{-1}), yeast extract (5 g L^{-1}), NaCl (10 g L^{-1}), agar 15% w/v and ampicillin (100 µg mL^{-1}) at pH 7.0; 37 °C for 24 h. Five isolated colonies were inoculated in 8 mL of LB (Difco, Detroit MI, USA) containing tryptone (10 g L^{-1}), yeast extract (5 g L^{-1}), NaCl (10 g L^{-1}) and ampicillin (100 µg L^{-1}); which was incubated in a shaker Excella® E24 (New Brunswick, New Jersey, USA), at 37 °C and 250 rpm for 8 h. For stock cultures, samples were withdrawn and glycerol was added to a final concentration of 15% (v/v) under sterile conditions and stored at −80 °C. The inoculum was prepared from 0.25 mL of the stock culture in 25 mL of LB (1:10, medium volume:flask volume ratio), at 37 °C and 250 rpm for 12 h. Culture for periplasmatic ASNase production was prepared from 0.5 mL of the inoculum in 25 mL (1:10, medium volume:flask volume ratio) of modified LB (addition of 0.1 mol L^{-1} of potassium phosphate buffer pH 7.0; 5.0 g L^{-1} of glucose; 0.5 g L^{-1} of $MgSO_4.7H_2O$; 0.05 g L^{-1} of $CaCl_2.2H_2O$; 0.1 mg L^{-1} of H_3BO_4; 0.1 mg L^{-1} of $CoCl_2.6H_2O$; 25 mg L^{-1} of $ZnSO_4.7H_2O$; 4 mg L^{-1} of $MnCl_2.4H_2O$; 0.1 mg L^{-1} of $NaMoO_4.2H_2O$; 1.8 mg L^{-1} of $CuSO_4.5H_2O$; 20 mg L^{-1} of $FeSO_4.7H_2O$; 0.1 mg L^{-1} of $NiSO_4.6H_2O$; 0.8% w/v of glycine and 6% v/v of n-dodecane) in a shaker at 37 °C and 250 rpm. After 4 h of growth, culture was induced for 24 h by 0.1 mmol L^{-1} of isopropyl β-D-thiogalactopyranoside (IPTG). A crude enzyme extract (cell-free supernatant) was obtained by centrifugation (10 000 × *g*, 4 °C and 5 min) and stored at −20 °C for further purification experiments. The crude enzyme extract presented protein concentrations of 4.3 ± 1.5 mg mL^{-1} and specific activity of 0.18 ± 0.05 U mg^{-1} protein.

Pre-purification step: enzyme precipitation by ammonium sulfate

A crude enzyme extract volume of 0.3 mL and 0.7 mL of saturated ammonium sulfate (70 wt%) was mixed for 2 min in a vortex mixer. Precipitated proteins were then removed by centrifugation (15000 × *g*, 15 min, 4 °C); the supernatant was discarded and the protein pellet was dissolved in 0.3 mL of distilled water.

Tie-lines (TLs) determined for the polymer–salt ATPS

Before the purification assays, tie-lines (TLs) for the polymer–salt ATPS were determined. The ternary phase diagram of

PEG 6000/citrate system at pH = 7 was obtained from literature,[34] and it was correlated using the Merchuk equation[38] (Equation (1)):

$$w_{PEG} = A \exp\left[\left(B\left[w_{Cit}\right]^{0.5}\right) - \left(C\left[w_{Cit}\right]^{3}\right)\right] \quad (1)$$

where w_{PEG} and w_{Cit} are, respectively, the polymer and inorganic salt weight percentages (wt%), and *A*, *B* and *C* are the Merchuk parameters.

The TLs were determined by a gravimetric method originally proposed by Merchuk *et al.*[38] to calculate the composition of the two-phases in equilibrium. The *TLs* were calculated for the system based in PEG 6000/citrate buffer at pH = 7, and considering the following extraction points (PEG/salt – wt%): 15/15; 17.5/17.5; 20/20 and 22.5/22.5. The weight compositions of both phase formers (PEG and citrate) in the top and bottom phases (w_{PEG}^{Top}, w_{Clt}^{Top}, w_{PEG}^{Bot}, w_{Cit}^{Bot}) were obtained by solving the following system of four equations and four unknown variables:

$$w_{PEG}^{Top} = Aexp[\left(B.w_{Cit}^{Top^{0.5}}\right) - \left(C.w_{Cit}^{Top^{3}}\right) \quad (2)$$

$$w_{PEG}^{Bot} = Aexp[\left(B.w_{Cit}^{Bot^{0.5}}\right) - \left(C.w_{Cit}^{Top^{3}}\right) \quad (3)$$

$$w_{PEG}^{TOP} = \frac{100\, w_{PEG}^{M}}{\alpha} - \frac{1-\alpha}{\alpha} w_{PEG}^{Bot} \quad (4)$$

$$w_{Cit}^{TOP} = \frac{100\, w_{Cit}^{M}}{\alpha} - \frac{1-\alpha}{\alpha} w_{Cit}^{Bot} \quad (5)$$

The superscripts *Top* and *Bot* designate the PEG 6000-rich and citrate-rich phases, respectively, and *M* represents the initial mixture point composition. The parameter α is the ratio between the top weight and total weight of the mixture. The solution of the referred system gives the concentration of the polymer and salt in the top and bottom phases. The tie-line length (*TLL*) is defined as:

$$TLL = \sqrt{\left(w_{Cit}^{Top} - w_{Cit}^{Bot}\right)^{2} + \left(w_{PEG}^{Top} - w_{PEG}^{Bot}\right)^{2}} \quad (6)$$

ASNase partition in ATPS

Polymer–salt ATPS composed of PEG and citrate, with and without the addition of ILs as adjuvants were prepared. In the studied ATPS, the top phase corresponds to the PEG-rich phase, while the bottom phase is mainly composed of the buffered salt. The ternary mixture compositions for ASNase purification were chosen based on the phase diagrams[34] constituted by PEGs with different molecular weights (2000, 4000, 6000 and 8000 g mol^{-1}) and the citrate buffer at different pHs (5, 6, 7 and 8). All phase formers were added into an Eppendorf flask as a dry powder or stock solution, along with 0.4 mL of crude extract of ASNase, resulting in a 2.0 g system. Each mixture was then stirred in a vortex mixer and left to equilibrate for 120 min (a period of time established in previous optimization experiments) at 4 °C in order to achieve the complete partition of ASNase between both phases. The volume of each phase, as well as ASNase activity and total protein concentration, were the parameters to determine. All experiments were carried out in triplicate and the interference of the buffer and PEG ascertained with the use of blank control samples, these prepared without the addition of ASNase crude extract. The partition coefficient of total proteins (K_P) was calculated as the ratio between the protein concentration in top and bottom phases, respectively, $[P]_t$ and $[P]_b$ according to Equation (7):

$$K_P = \frac{[P]\,t}{[P]\,b} \quad (7)$$

The partition coefficient of ASNase (K_A) was calculated as the ratio between the volumetric activity of ASNase (U mL^{-1}) in the top (At) and bottom phases (Ab), according to Equation (8):

$$K_A = \frac{At}{Ab} \quad (8)$$

The recovery yields of total proteins (%Rec P) and ASNase (%Rec A) into to PEG-rich phase were defined based on the partition coefficients of total proteins and ASNase, respectively, and the volume ratio (Vr), according to Equation (9):

$$\%RecP\ or\ A = \frac{100}{\left(1 + \left(\frac{1}{Vr \times Kp\ or\ A}\right)\right)} \quad (9)$$

The purification factor (PF) is given by the ratio between the specific activity of the top phase (SA_t) and the specific activity of the initial crude enzyme extract (SAi), according to Equation (10):

$$PF = \frac{SAt}{SAi} \quad (10)$$

In situ extraction of ASNase: pre-purification and purification steps

The *in situ* extraction of ASNase from *E. coli* was performed through cell permeabilization by glycine and *n*-dodecane, followed by the contaminant proteins' precipitation with ammonium sulfate. After the precipitation step, ATPS (with and without ILs as adjuvants) were integrated as a final step of purification. The ATPS used in this downstream process were the PEG 6000/citrate buffer (15/15 wt%) at pH = 7 without IL and PEG 6000/citrate buffer (15/15 wt%) with 5 wt% of $[C_4mim][CH_3SO_3]$ as adjuvant at pH = 7 for the ATPS supplemented with IL.

Determination of ASNase activity

The ASNase activity was based on the protocol of Drainas and co-workers[30] and expressed as IU mL^{-1}. Briefly, 0.1 mL of sample, 0.7 mL of of Tris–HCl buffer (50 mmol L^{-1}, pH 8.6), 0.1 mL of L-asparagine (0.1 mol L^{-1}) and 0.1 mL of hydroxylamine (1.0 mol L^{-1}, pH 7.0) were incubated at 37 °C for 30 min. The reaction was interrupted by adding 0.5 mL of 0.31 mol L^{-1} of iron chloride reagent (dissolved in HCl 0.33 mol L^{-1} and trichloroacetic acid 0.3 mol L^{-1} solution). The reaction solution was centrifuged at 3220 × *g* for 15 min and the iron chloride–hydroxamic acid complex produced was quantified at 500 nm. The calibration curve was prepared from a β-aspartohydroxamic solution (Sigma-Aldrich, MO, USA). In this work, one unit of ASNase activity is defined as the amount of enzyme that produces 1 µmol of β-aspartohydroxamic acid per minute under the experiment conditions defined. The specific activity (U mg^{-1}) represents the ratio between the volumetric activity of ASNase (U mL^{-1}) and the total protein concentration (mg mL^{-1}).

Table 1. Effect of polymer molecular mass, pH, phase composition and adjuvant concentration on the partition behaviour of ASNase through the use of *in situ* polymer-citrate buffer ATPS

			Phase composition (wt%)								
No.	Polymer	pH	PEG	Citrate	Water	Adjuvant; Concentration (wt%)	K_P	K_A	%Rec P	%Rec A	PF
1	PEG 2000	7	15	15	70		2.40 ± 0.26	3.09 ± 0.15	61.37 ± 0.16	67.27 ± 1.05	2.14 ± 0.13
2	PEG 4000	7	15	15	70		1.99 ± 0.03	7.91 ± 0.15	54.60 ± 0.16	82.35 ± 2.07	4.76 ± 0.53
3	PEG 6000	7	15	15	70		2.36 ± 0.14	25.59 ± 0.15	58.72 ± 0.16	93.71 ± 1.05	13.45 ± 1.61
4	PEG 8000	7	15	15	70		2.96 ± 0.32	25.57 ± 3.15	63.80 ± 3.16	93.86 ± 0.31	8.73 ± 0.10
5	PEG 6000	5	15	15	70		2.28 ± 0.71	20.47 ± 1.32	59.24 ± 1.27	91.56 ± 1.25	12.55 ± 1.12
6	PEG 6000	6	15	15	70		2.24 ± 0.45	18.75 ± 0.45	58.26 ± 2.03	90.81 ± 0.32	12.68 ± 1.20
7	PEG 6000	8	15	15	70		4.09 ± 1.16	5.66 ± 1.16	70.19 ± 6.01	92.04 ± 2.64	6.42 ± 2.15
8	PEG 6000	7	17.5	17.5	65		2.36 ± 0.34	7.01 ± 1.00	56.27 ± 2.51	80.51 ± 2.25	7.37 ± 0.18
9	PEG 6000	7	20	20	60		6.56 ± 1.13	17.25 ± 5.60	81.51 ± 0.28	90.35 ± 2.86	6.87 ± 1.36
10	PEG 6000	7	22.5	22.5	55		9.74 ± 0.51	30.22 ± 9.92	85.36 ± 0.80	97.73 ± 0.30	9.67 ± 0.07
11	PEG 6000	7	15	15	69	$[C_4mim]Cl$; 1 wt%	2.43 ± 0.55	26.36 ± 0.25	60.95 ± 1.67	94.05 ± 0.24	13.86 ± 0.41
12	PEG 6000	7	15	15	69	$[C_4mim][DMP]$; 1 wt%	3.91 ± 0.49	18.37 ± 1.30	69.32 ± 3.26	91.65 ± 0.54	9.66 ± 0.68
13	PEG 6000	7	15	15	69	$[C_4mim][CH_3SO_3]$; 1 wt%	2.09 ± 0.18	32.06 ± 0.76	55.19 ± 0.43	95.06 ± 0.11	16.85 ± 0.40
14	PEG 6000	7	15	15	69	$[C_4mim][CF_3SO_3]$; 1 wt%	2.42 ± 0.01	31.02 ± 0.15	59.19 ± 0.16	94.90 ± 0.02	16.30 ± 0.08
15	PEG 6000	7	15	15	67.5	$[C_4mim][CH_3SO_3]$; 2.5 wt%	2.21 ± 0.43	24.78 ± 1.32	57.01 ± 1.39	91.94 ± 0.02	18.85 ± 1.02
16	PEG 6000	7	15	15	65	$[C_4mim][CH_3SO_3]$; 5 wt%	1.21 ± 0.12	22.08 ± 3.02	40.37 ± 1.14	87.94 ± 0.03	20.09 ± 0.35

Determination of total protein concentration

The protein concentration was determined with the Pierce BCA Protein Assay and Micro BCA Protein Assay (Thermo Scientific, Schwerte, Germany) according to the product recommendations. Bovine serum albumin was used as standard protein.

In silico analysis

Escherichia coli ASNase structure (code 3ECA)[39] was retrieved from the Protein Data Bank (PDB) and converted into PQR files according to Dolinsky *et al.*[40] using PARameters for Solvation Energy (PARSE) force field at different pH values (5, 6, 7 and 8). A PQR file is a PDB file with the temperature and occupancy columns replaced by columns containing the per-atom charge (Q) and radius (R). Electrostatic properties were calculated using automatically-configured sequential focusing multigrid calculation on Adaptive Poisson-Boltzmann Solver (APBS). These systems can model biomolecular solvation by solving the Poisson–Boltzmann equation (PBE). Moreover, these will also provide implicit solvent models of nonpolar solvation, which accurately account for both repulsive and attractive solute–solvent interactions. Hydrophobicity was estimated by the software ExPasy[41] (adapted to red scale), which is based on amino acid scale from Eisenberg *et al.*[42] All results were performed using PyMOL Molecular Graphics System, Version 1.8 Schrödinger, LLC.

RESULTS AND DISCUSSION

Preparation of the ASNase crude extract

After the *E. coli* cultivation (see Methods section) and ASNase expression, the cell disruption was promoted by using glycine and *n*-dodecane. From this procedure, the complete secretion of periplasmatic ASNase was achieved, however, other proteins were also released. Chemical permeabilization of outer cell membrane with detergents and salts, such as Triton X-100 and K_2HPO_4, is reported in literature for ASNase secretion from *E. coli*.[21] However, this is the first time that glycine (for the disruption of the peptidoglycan layer)[43] and *n*-dodecane (for the disruption of the outer cell membrane)[44] are employed together in an integrated purification process using ATPS. This permeabilization approach was previously studied and proved to be effective for enzyme release, with 89% of ASNase secreted to fermentation broth.[45] The final crude enzyme extract obtained has a protein concentration of 4.3 ± 1.5 mg mL^{-1} and specific activity of 0.18 ± 0.05 U mg^{-1} protein.

ASNase partition in polymer-salt ATPS

Polymer–salt ATPS were studied in the purification of ASNase from crude enzyme extract. Ternary phase diagrams described in the literature[34] were used to determine the extraction mixture compositions. Commonly, polymer/phosphate buffer-based ATPS are focused, however in this work, a citrate buffer-based salt was used, since this is more biocompatible and biodegradable. In addition, this buffer is able to maintain the pH stable over a wider range and to create a larger biphasic region to work in, due to its stronger salting-out ability. Table 1 summarizes all ASNase partition results obtained by applying *in situ* polymer–salt ATPS, considering the study of several conditions. It should be stressed that no protein precipitation was observed in any experimental condition and the protein mass balance was acceptably in the range 80–120%. Given the high number of systems and conditions tested, this work will be mainly discussed considering each one of the conditions individually.

ASNase partition in PEG/citrate buffer-based ATPS

Usually, the partition coefficient of proteins (K_P) depends on several factors, such as the characteristics of the phase-forming polymer, the hydrophobic effect, charge and size of proteins. The partition coefficient of the target protein (K_A) is mostly dependent on the specific characteristics of the enzyme that could lead to interactions with the phase formers, e.g. hydrophobicity, hydrophilicity, charge or π-interacting groups.

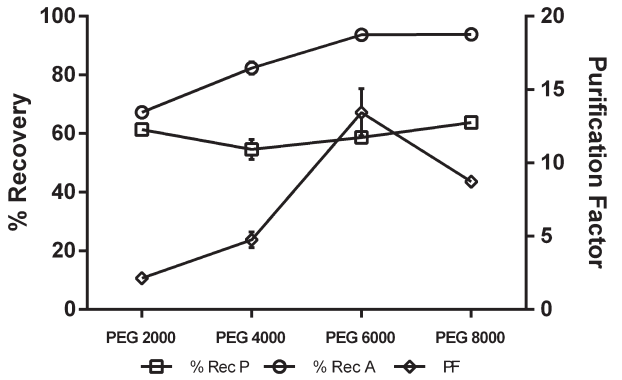

Figure 1. Recovery yield of total proteins (%Rec P) and ASNase (%Rec A) and purification factor of ASNase (PF) for the ATPS composed of PEG + citrate buffer (15 wt%/15 wt%) at pH 7. Errors bars correspond to standard deviations obtained from three replicates.

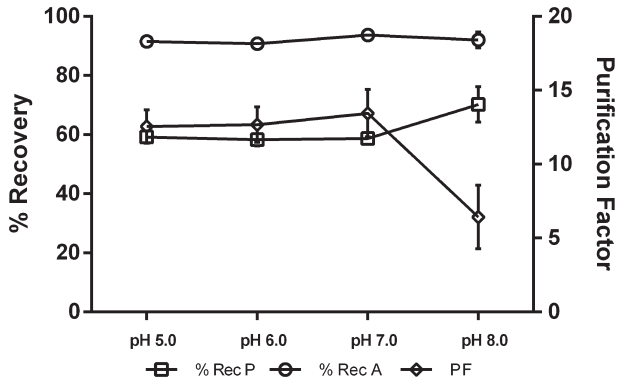

Figure 2. Recovery yield of total proteins (%Rec P) and ASNase (%Rec A), and purification factor of ASNase (PF) for the ATPS composed of PEG 6000 + citrate buffer (15 wt%/15 wt%) at different pHs. Error bars correspond to standard deviations obtained from three replicates.

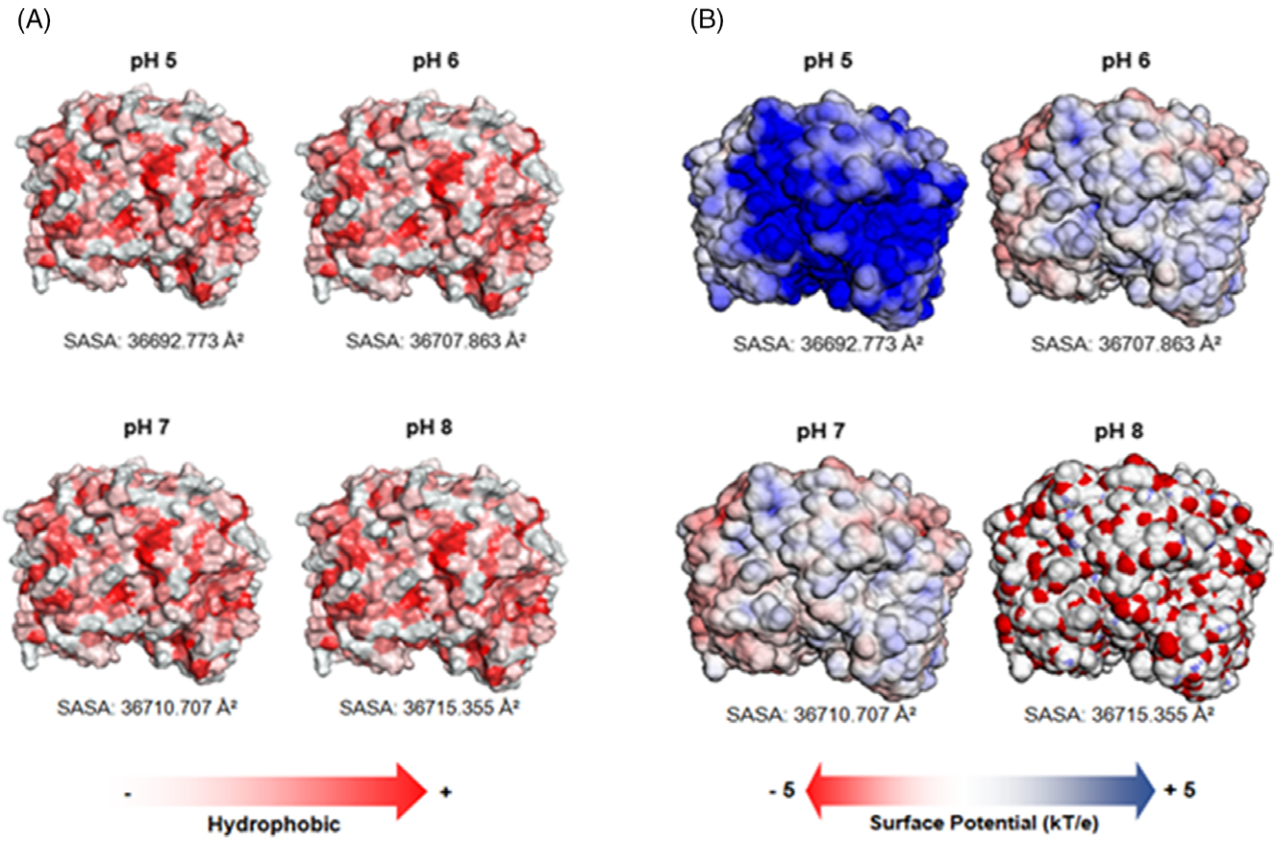

Figure 3. 3D structure of ASNase (PDB: 3ECA) (A) hydrophobicity surface using Eisenberg amino acid scale[39] and solvent-accessible surface area (SASA), calculated for pHs 5, 6, 7 and 8. Red-scale refers to less hydrophobic (white) to more hydrophobic (red) parts of ASNase; (B) electrostatic charge at the ASNase surface and solvent-accessible surface area (SASA) calculated for pHs 5 to 8. Red-white-blue scale refers to minimum (-5 kT/e, red) and maximum (5 kT/e, blue) surface potential.

The recovery yields, %Rec A and %Rec P, and purification factors of ASNase in ATPS composed of PEGs with different molecular weight + citrate buffer (at pH = 7) are presented in Fig. 1. All mixtures compositions used in this set of experiments correspond to the same extraction point composed of 15 wt% of polymer +15 wt% of citrate buffer +70 wt% of water. As can be seen, the ASNase partitions preferentially to the polymer-rich phase and this tendency increases with the polymer molecular weight. From the partition coefficient data, it is concluded that the ASNase partition suffers the highest variations when different polymer molecular weights are tested, which is demonstrated by the greatest variation of K_A (from 3.09 ± 0.15 to 25.59 ± 0.15) when compared with K_P range (from 1.99 ± 0.03 to 2.96 ± 0.32). The ASNase partition results from the combined citrate salting-out effect and hydrophobic interactions between PEG and the hydrophobic parts of ASNase, reported in the literature by Sanches and collaborators.[46] In addition, recent studies identified the same partition trend for ASNase in PEG 1000, 3000, 6000/potassium dihydrogen phosphate

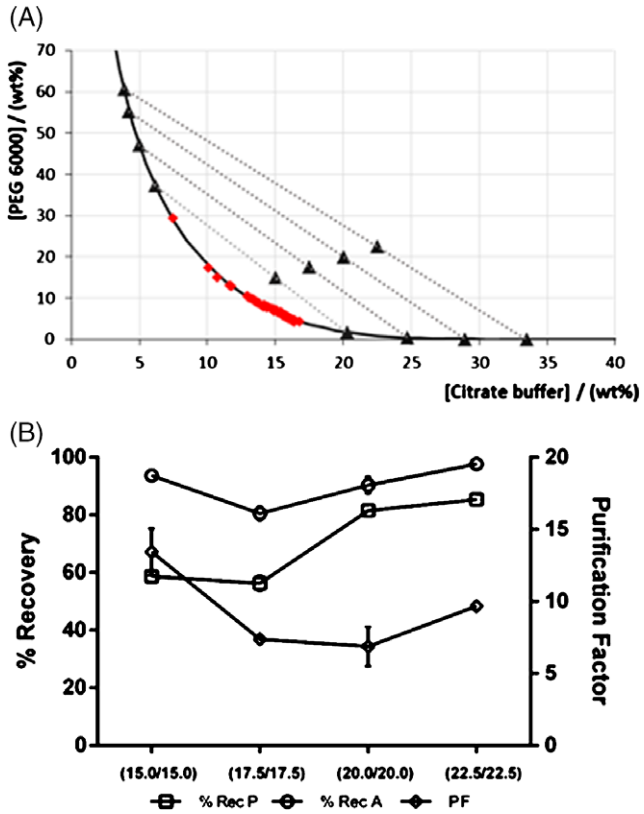

Figure 4. (A) Ternary phase diagram of PEG 6000 + citrate buffer system at pH = 7 with representation of tie-lines (TL) for the following mixture points: PEG 6000 wt%/citrate buffer wt% = 15.0/15.0; 17.5/17.5; 20.0/20.0; 22.5/22.5. (B) Recovery yields of total proteins (%Rec P) and ASNase (%Rec A) and purification factor (PF) for the PEG 6000 + citrate buffer ATPS at pH = 7, considering four distinct mixture points. Error bars correspond to standard deviations obtained from three replicates.

ATPS.[17] This can justify the increase of %Rec A (from 67.27 ± 1.05 to 93.86 ± 0.31%) and K_A (from 3.09 ± 0.15 to 25.59 ± 0.15) by increasing the polymer molecular weight. In terms of total proteins, a different partition behaviour was observed, since PEGs of intermediate molecular mass (4000 and 6000) presented a lower tendency to concentrate contaminant proteins in PEG-top rich phase (Fig. 1 and Table 1). Nevertheless, the higher PF was observed for PEG 6000, resulting from the high K_A (25.59 ± 0.15) and %Rec A (similar to PEG 8000-based ATPS) and one of the lowest K_P (2.36 ± 0.14) and %Rec P values (%Rec P = 58.72 ± 0.16%). Taking into consideration the overall set of results obtained for the purification parameters of ASNase, the PEG 6000-based ATPS was selected for further studies.

The recovery yields, %Rec A and %Rec P and purification factors of ASNase in ATPS composed of PEG 6000/citrate buffer at different pH values are presented in Fig. 2. It is observed that through the change of pH, the partition of ASNase continues to be mostly dominated by hydrophobic interactions, since high %Rec A are obtained towards the polymer-rich phase.[17] In this sense, *in silico* studies performed to characterize the hydrophobic regions of ASNase, at different pH values, are presented in Fig. 3(A). The analysis of the solvent-accessible surface area (SASA) shows a significant hydrophobic region on the ASNase surface that does not change significantly with pH. Compared with conventional hydrophilic proteins with a size similar to ASNase, human serum albumin (1BM0, HSA)[47] – 57412.180 A^2 and bovine serum albumin (4F5S, BSA)[48] – 58218.199 A^2, it is found that the low SASA values of ASNase confirm its hydrophobic character. Previous results[17] reported an increase of the ASNase partition towards the PEG-rich phase at pH close to the p*I* (pI = 4.9)[17,18] by the application of PEG/phosphate-based ATPS, as a result of the electrostatic interactions reduction between cell debris and the product molecules. From the data gathered, it was inferred that pH does not affect significantly the ASNase SASA values, nor its partition behaviour in PEG/citrate-based ATPS, reinforcing the hypothesis that hydrophobic interactions are the important driving-force in polymer/salt-based ATPS. However, in aqueous solution pH affects the electric charges of both ASNase (Fig. 3(B)) and periplasmatic (contaminant) proteins, thus influencing the protein partition between both phases. The recovery of total proteins (%Rec P) in the PEG-rich phase increased in alkaline pH values (pH = 8), therefore, leading to a decrease in PF. After optimization of the pH, the system PEG 6000/citrate buffer at pH = 7 was considered as the most efficient and used in further studies, comprising the effect of the mixture point/TLL and the use of ILs as adjuvants.

Figure 4 shows the results of four mixture points (15.0/15.0; 17.5/17.5; 20.0/20.0; 22.5/22.5 wt% of polymer/salt) studied for the PEG 6000/citrate buffer system at pH 7. The composition of the top polymer-rich phase and bottom salt-rich phase, along with the parameter α and tie-line length (*TLL*) for each studied ATPS are presented in Table 2. From the results obtained, it is concluded that higher *TLL*s were obtained for the systems with higher amounts of both phase formers. Moreover, the partition of the total proteins seems to be dependent on the TLL since there is an increase of K_P (*c.* 4.1-fold) and %Rec P (*c.* 20% higher) with increase of *TLL* (Fig. 4(B) and Tables 1 and 2). The citrate content present in the bottom rich-phase ranged from 20.26 to 33.50 wt% (Table 2), resulting in a stronger salting-out effect for higher *TLL*. These results show that while hydrophobic interactions are again dominating the partition of ASNase, for the more hydrophilic contaminant periplasmatic proteins, their partition is being dominated by the salting-out effects. It is thus possible to use these distinct driving-force mechanisms of partition of both ASNase and periplasmatic contaminant proteins to manipulate the purification of ASNase. After optimization of the TLL effect, it was defined as the best condition the lowest TLL (TLL = 38.33), represented by the

Table 2. Composition of the initial mixture point (M), polymer-rich phase (Top) and salt-rich. phase (Bot), along with the parameter α and the tie-line length (*TLL*).

$[PEG]^M$	$[Cit]^M$	$[PEG]^{Top}$	$[Cit]^{Top}$	$[PEG]^{Bot}$	$[Cit]^{Bot}$	α	*TLL*
15.0	15.0	37.36	6.15	1.72	20.26	0.373	38.33
17.5	17.5	47.10	4.99	0.37	24.74	0.366	50.72
20.0	20.0	55.25	4.24	0.061	28.91	0.361	60.45
22.5	22.5	60.70	3.88	0.0042	33.50	0.371	66.94

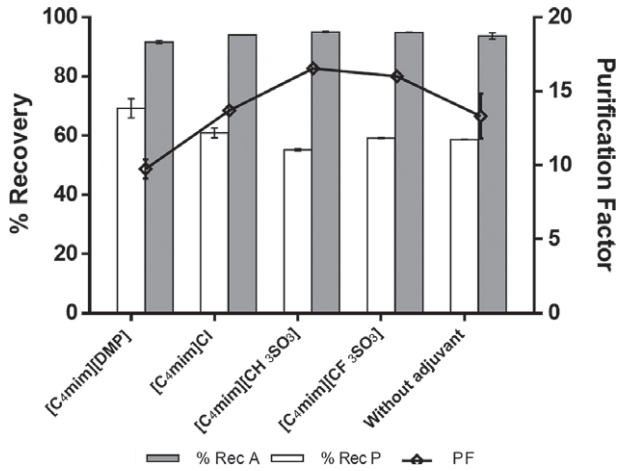

Figure 5. Recovery yield of total proteins (%Rec P) and ASNase (%Rec A), and purification factor (PF) in the ATPS composed of PEG 6000 + citrate buffer (15 wt%/15 wt%) at pH = 7 and with 1 wt% of [C_4mim]-based ILs as adjuvants. Error bars correspond to standard deviations obtained from three replicates.

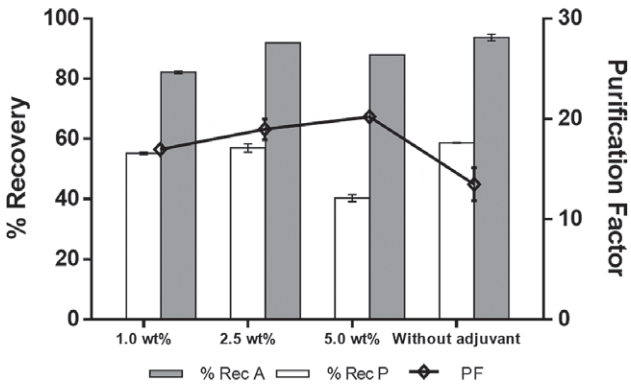

Figure 6. Recovery yield of total proteins (%Rec P) and ASNase (%Rec A) and purification factor (PF) in the ATPS composed PEG of 6000 + citrate buffer (15 wt%/15 wt%) at pH = 7 and with [C_4mim][CH_3SO_3] as adjuvant. Errors bars correspond to standard deviations obtained from three replicates.

mixture point composed of 15 wt% of PEG 6000/15 wt% of citrate buffer at pH 7.0, with %Rec A > 80%, K_A > 7, and PF = 13.45 ± 1.61. This extraction point was then adopted to investigate the effect of ILs as adjuvants on the ASNase purification.

ASNase partition in PEG + citrate buffer + IL (as adjuvant)-based ATPS

The study of the effect of the ILs as adjuvants in the purification of enzymes produced via fermentation was recently reported as being one of the most promising approaches to purification,[49] which was also adopted in this work. Herein, four ILs were tested as adjuvants, on ASNase partition, in concentrations of 1 wt% of the overall system weight. Four imidazolium-based ILs presenting the same cation ([C_4mim]$^+$) combined with the anions Cl^-, $[DMP]^-$, $[CH_3SO_3]^-$ and $[CF_3SO_3]^-$ were selected to evaluate the effect of their polarity on the partition of both ASNase and contaminant proteins. First, all imidazolium-based ILs investigated have a preferential partition towards the top phase, as reported elsewhere,[34] affecting the chemical and physical properties of the polymer-rich phase. According to the results reported in Fig. 5, no

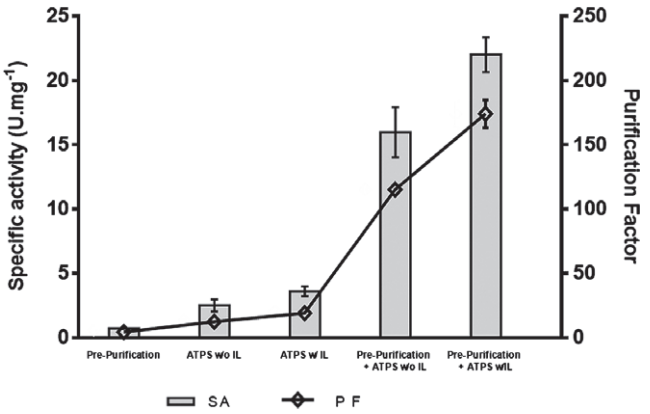

Figure 7. Results obtained for each purification strategy investigated in this work to efficiently separate ASNase from the contaminant proteins.

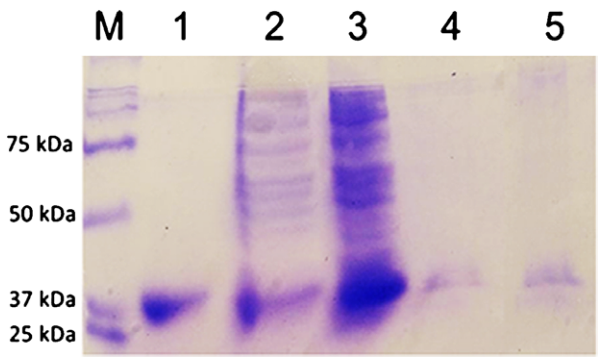

Figure 8. SDS-PAGE of commercial ASNase from *E. coli* (1) Precipitated proteins from fermentation broth. (2) Fermentation broth. (3) Top-phase of the optimized ATPS, the PEG 6000/citrate with 5 wt% [C_4mim][CH_3SO_3] (as adjuvant) with pre-purification. (4) Top-phase of the optimized ATPS, the PEG 6000/citrate with 5 wt% [C_4mim][CH_3SO_3] (as adjuvant) without pre-purification. (5) Molar masses reference Precision Plus Protein (BIORAD, CA, US) (M).

significant differences were observed in %Rec A, independently of the IL used. However, the data suggest that the ILs have an influence on the partition of the periplasmatic proteins, thus resulting in %Rec P ranging from 55.19 ± 0.43 to 69.32 ± 3.26%. The less polar anions, [C_4mim][CH_3SO_3] and [C_4mim][CF_3SO_3], by enhancing the hydrophobicity of the top phase, were found to effectively decrease the amount of contaminant proteins in the PEG 6000-rich phase, increasing the PF by approximately 20%. Moreover, the polar anions Cl^- and $[DMP]^-$ seem to reduce the hydrophobicity of the polymer-rich phase enhancing the partition of the periplasmatic proteins to this phase, thus reducing the PF. Summing up, ILs with higher polarity decreased the PF, meaning that specific polar interactions between the periplasmatic proteins and ILs are promoted in the top phase, enhancing the partition of the contaminant proteins towards the polymer-rich phase. Contrastingly, both [C_4mim][CH_3SO_3] and [C_4mim][CF_3SO_3] display lower hydrogen-bond basicity and were better at enhancing the ASNase PF, through the decrease of IL-contaminant proteins interactions. These results corroborate the importance of the IL anion in the partition of proteins, in this case, the contaminant periplasmatic proteins, thus allowing the increase of the purification performance of the polymeric ATPS. At this stage, the maximum purification achieved was around PF = 16.85 ± 0.40 for the [C_4mim][CH_3SO_3]. In order to endorse this

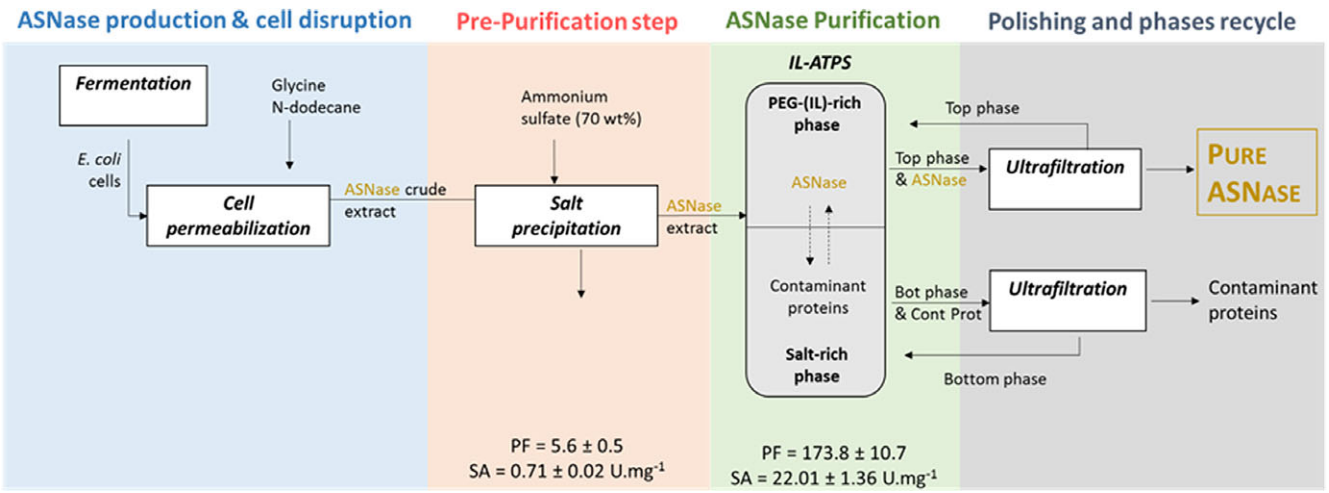

Figure 9. Schematic representation of the *in situ* purification process of periplasmatic ASNase using polymer-based ATPS with $[C_4mim][CH_3SO_3]$ as adjuvant. The isolation of ASNase and the recycling of both aqueous phases are also represented.

statement, and aiming to increase even more the PF of ASNase, the effect of IL concentration was studied, specifically for the $[C_4mim][CH_3SO_3]$ (best system). The results (Fig. 6) corroborated the tendency previously discussed; the increased concentration of this less polar IL significantly suppresses the partition of contaminant proteins towards the PEG-rich phase, culminating in the highest PF = 20.09 ± 0.35 obtained for the ATPS with 5 wt% of IL. In summary, small IL amounts' could enhance the ASNase partition and improve the purification performance of ATPS, which obviously brings additional advantages regarding enzyme purity and the cost of the overall process downstream.

In situ extraction of L-asparaginase by ATPS integrated with pre-purification step

Despite the good results for PF factor obtained, these are not sufficient for the use of ASNase as a biopharmaceutical. Therefore, a new strategy of purification was defined, which consists in the integration of two steps of purification. In this ambit, a pre-purification step was included between the stages of production and purification using the best-performing ATPS (15 wt% of PEG 6000 + 15 wt% of citrate buffer +65 wt% of water +5 wt% of $[C_4mim][CH_3SO_3]$ at pH = 7). The pre-purification was thus defined by using an ammonium sulfate solution to precipitate as much as possible the contaminant proteins, a strategy recurrently applied in the purification of enzymes.[49] The inclusion of a pre-purification step can help eliminate: (i) the contaminant proteins partitioned to the same aqueous phase as ASNase; and (ii) the antagonists and cell debris that may affect the ASNase activity. Moreover, some other advantages could be defined, like the fact that the ammonium sulfate precipitation is a cost-effective and scalable purification approach that could increase the overall purity of ASNase. Taking these advantages into account, different strategies/platforms were compared for the purification of ASNase (Fig. 7). Analysing the results of Fig. 7, the advantage of using the integration of both pre-purification and purification processes (ammonium sulfate precipitation + $[C_4mim][CH_3SO_3]$-based ATPS, respectively), gives an approach resulting in the highest purification performance. This integrated downstream process proved to be much more efficient with higher ASNase specific activity (22.0 ± 1.36 U mg^{-1} protein) and purification factor (PF = 174 ± 11) than the isolated purification step by itself (ATPS or protein precipitation). Figure 8 shows the SDS-PAGE profile of the different steps of purification (Lane 5) and of the integrated downstream process (Lane 4) developed in this work. Through the main results it is concluded that a clear band of the ASNase subunit is obtained (≈ 35 kDa) for the integrated process (Lane 4), with the absence of contaminant proteins. Actually, with the pre-purification step, the elimination of a diversified plethora and high content of contaminant periplasmatic proteins,[50] e.g. nucleotidases, β-lactamase, alkaline phosphatase, ribonuclease, endonuclease I, caboxypeptidase II, cytochrome c, hydrogenase and nitrite reductase, was possible, while maintaining the ASNase structural integrity and activity for further purification using ATPS.

Since the main aim of this work is the optimization of ASNase purification from the fermentation broth, the integrated downstream process envisaged is schematically represented as Fig. 9. This comprises the purification step, the cell disruption to release the ASNase, the pre-purification step to eliminate part of the contaminant proteins, the IL-ATPS to refine purification of the biopharmaceutical, and the isolation of ASNase. As depicted, the best ATPS and conditions selected are represented, as well as the isolation methods defined for the polishing of ASNase and contaminant proteins from both phases by using ultrafiltration, culminating in the sequential reuse of the phases in new cycles of purification.

CONCLUSIONS

In this work, an efficient integrated downstream process combining cell permeabilization (applying glycine and n-dodecane) with the purification of ASNase using IL-ATPS was demonstrated. Polymer-based ATPS using ILs as adjuvants were shown to be efficient in the purification of enzymes, i.e. ASNase. The results reveal the high affinity of ASNase for the polymer-rich phase of the ATPS, justified by the hydrophobic interactions established between the enzyme and the polymer. The high purification performance of the ATPS was demonstrated using 5 wt% of $[C_4mim][CH_3SO_3]$ as adjuvant (when compared with the common polymeric system), attaining a PF of 20.09 ± 0.35 and SA of 3.33 ± 0.38 U mg^{-1} protein. Taking into account other purification schemes, an ammonium precipitation pre-purification step was tested, demonstrating again clear advantages in terms of downstream process efficiency over discrete and sequential operations, attaining a purification

factor of 173.8 ± 10.7. It was shown that low amounts of ILs in the formulation of ATPS were enough to achieve complete extractions of ASNase (%Rec ASNase ≈ 90%) with high purity. The system with high purification performance was then used in the design of an integrated process comprising the steps production, cell disruption, and purification with an ammonium sulfate precipitation followed by the application of ATPS with IL as adjuvant, and culminating in the ASNase isolation and reuse of the various phases.

ACKNOWLEDGEMENTS

This work was developed within the scope of the project CICECO-Aveiro Institute of Materials, POCI-01-0145-FEDER-007679 (FCT Ref. UID/CTM/50011/2013), financed by national funds through the FCT/MEC and when appropriate co-financed by FEDER under the PT2020 Partnership Agreement. The authors are grateful for the financial support of Portuguese Foundation for Science and Technology (FCT) for the doctoral grant SFRH/BD/102915/2014 of João H. P. M. Santos. S.P.*M. Ventura* acknowledges FCT/MEC for a contract under *Investigador FCT* 2015 contract number IF/00402/2015. The authors also thank FAPESP (São Paulo Research Foundation, Brazil) for the financial support through the project process 2013/08617-7 and CNPq (National Council for Scientific and technological Development, Brazil).

REFERENCES

1 Soares AL, Guimarães GM, Polakiewicz B, Pitombo RNDM and Abrahão-Neto J, Effects of polyethylene glycol attachment on physicochemical and biological stability of *E. coli* L-asparaginase. *Int J Pharm* **237**:163–170 (2002).
2 van den Berg H, Asparaginase revisited. *Leuk Lymphoma* **52**:168–178 (2011).
3 Piatkowska-Jakubas B, Krawczyk-Kuliś M, Giebel S, Adamczyk-Cioch M, Czyz A, Lech Marańda E *et al.*, Use of L-asparaginase in acute lymphoblastic leukemia: recommendations of the Polish Adult Leukemia Group. *Pol Arch Med Wewn* **118**:664–669 (2008).
4 Rizzari C, Conter V, Starý J, Colombini A, Moericke A and Schrappe M, Optimizing asparaginase therapy for acute lymphoblastic leukemia. *Curr Opin Oncol* **25**:S1–S9 (2013).
5 Pui CH, Robison LL and Look AT, Acute lymphoblastic leukaemia. *Lancet* **371**:1030–1043 (2008).
6 Schleis SE, Rizzo SA, Phillips JC and LeBlanc AK, Asparaginase-associated pancreatitis in a dog. *Can Vet J* **52**:1009–1012 (2011).
7 Beard ME, Crowther D, Galton DA, Guyer RJ, Fairley GH, Kay HE *et al.*, L-asparaginase in treatment of acute leukaemia and lymphosarcoma. *Br Med J* **1**:191–195 (1970).
8 DeVita VT and Chu E, A history of cancer chemotherapy. *Cancer Res* **68**:8643–8653 (2008).
9 WHO, WHO | WHO Model Lists of Essential Medicines. *World Heal Organ* **19**:55 (2015).
10 Narta UK, Kanwar SS and Azmi W, Pharmacological and clinical evaluation of l-asparaginase in the treatment of leukemia. *Crit Rev Oncol/Hematol* **61**:208–221 (2007).
11 Bierau H, Hinton RJ and Lyddiatt A, Direct process integration of cell disruption and fluidised bed adsorption in the recovery of labile microbial enzymes. *Bioseparation* **10**:73–85 (2001).
12 Krasotkina J, Borisova AA, Gervaziev YV and Sokolov NN, One-step purification and kinetic properties of the recombinant L-asparaginase from Erwinia carotovora. *Biotechnol Appl Biochem* **39**:215–221 (2004).
13 Kumar S, Venkata Dasu V and Pakshirajan K, Purification and characterization of glutaminase-free l-asparaginase from *Pectobacterium carotovorum* MTCC 1428. *Bioresource Technol* **102**:2077–2082 (2011).
14 Badoei-Dalfard A, Purification and characterization of l-asparaginase from Pseudomonas aeruginosa strain SN004: production optimization by statistical methods. *Biocatal Agric Biotechnol* **4**:388–397 (2015).
15 Dharmaraj S, Study of L-asparaginase production by *Streptomyces noursei* MTCC 10469, isolated from marine sponge Callyspongia diffusa. *Iran J Biotechnol* **9**:102–108 (2011).
16 Upadhyay AK, Singh A, Mukherjee KJ and Panda AK, Refolding and purification of recombinant L-asparaginase from inclusion bodies of *E. coli* into active tetrameric protein. *Front Microbiol* **5**:486 (2014).
17 Zhu JH, Yan XL, Chen HJ and Wang ZH, *In situ* extraction of intracellular l-asparaginase using thermoseparating aqueous two-phase systems. *J Chromatogr A* **1147**:127–134 (2007).
18 Khushoo A, Pal Y, Singh BN and Mukherjee KJ, Extracellular expression and single step purification of recombinant *Escherichia coli* L-asparaginase II. *Protein Expr Purif* **38**:29–36 (2004).
19 Kim SK, Min WK, Park YC and Seo JH, Application of repeated aspartate tags to improving extracellular production of *Escherichia coli* l-asparaginase isozyme II. *Enzyme Microbiol Technol* **79–80**:49–54 (2015).
20 Khushoo A, Pal Y and Mukherjee KJ, Optimization of extracellular production of recombinant asparaginase in *Escherichia coli* in shake-flask and bioreactor. *Appl Microbiol Biotechnol* **68**:189–197 (2005).
21 Qin M and Zhao F, L-asparaginase release from *Escherichia coli* cells with aqueous two-phase micellar systems. *Appl Biochem Biotechnol* **110**:11–21 (2003).
22 Hernandez-Justiz O, Fernandez-Lafuente R, Terreni M and Guisan JM, Use of aqueous two-phase systems for *in situ* extraction of water soluble antibiotics during their synthesis by enzymes immobilized on porous supports. *Biotechnol Bioeng* **59**:73–79 (1998).
23 Azevedo AM, Rosa PAJ, Ferreira IF and Aires-Barros MR, Optimisation of aqueous two-phase extraction of human antibodies. *J Biotechnol* **132**:209–217 (2007).
24 Viana Marques DA, Pessoa-Júnior A, Lima-Filho JL, Converti A, Perego P and Porto ALF, Extractive fermentation of clavulanic acid by Streptomyces DAUFPE 3060 using aqueous two-phase system. *Biotechnol Prog* **27**:95–103 (2011).
25 Rito-Palomares M, Nuez L and Amador D, Practical application of aqueous two-phase systems for the development of a prototype process for c-phycocyanin recovery from Spirulina maxima. *J Chem Technol Biotechnol* **76**:1273–1280 (2001).
26 Rito-Palomares M and Middelberg AP, Aqueous two-phase systems for the recovery of a recombinant viral coat protein from *Escherichia coli*. *J Chem Technol Biotechnol* **77**:1025–1029 (2002).
27 Liu X, Mu T, Sun H, Zhang M and Chen J, Optimisation of aqueous two-phase extraction of anthocyanins from purple sweet potatoes by response surface methodology. *Food Chem* **141**:3034–3041 (2013).
28 Rito-Palomares M, Negrete A, Miranda L, Flores C, Galindo E and Serrano-Carreón L, The potential application of aqueous two-phase systems for *in situ* recovery of 6-pentyl-infinity-pyrone produced by *Trichoderma harzianum*. *Enzyme Microbiol Technol* **28**:625–631 (2001).
29 Imada A, Igarasi S and Nakahama K, Asparaginase and glutaminase activities of micro-organisms. *Microbiology* **76**:85–89 (1973).
30 Drainas C and Pateman JA, L-Asparaginase activity in the fungus *Aspergillus nidulans*. *Biochem Soc Trans* **5**:259–261 (1977).
31 Hapiot P and Lagrost C, Electrochemical reactivity in room-temperature ionic liquids. *Chem Rev* **108**:2238–2264 (2008).
32 Freire MG, Cláudio AFM, Araújo JMM, Coutinho JAP, Marrucho IM, Lopes JNC *et al.*, Aqueous biphasic systems: a boost brought about by using ionic liquids. *Chem Soc Rev* **41**:4966 (2012).
33 Pereira JFB, Lima ÁS, Freire MG and Coutinho JAP, Ionic liquids as adjuvants for the tailored extraction of biomolecules in aqueous biphasic systems. *Green Chem* **12**:1661 (2010).
34 Ferreira AM, Faustino VFM, Mondal D, Coutinho JAP and Freire MG, Improving the extraction and purification of immunoglobulin G by the use of ionic liquids as adjuvants in aqueous biphasic systems. *J Biotechnol* **236**:166–175 (2016).
35 de Souza RL, Campos VC, Ventura SPM, Soares CMF, Coutinho JAP and Lima ÁS, Effect of ionic liquids as adjuvants on PEG-based ABS formation and the extraction of two probe dyes. *Fluid Phase Equilib* **375**:30–36 (2014).
36 Santos JHPM, e Silva FA, Coutinho JAP, Ventura SPM and Pessoa A, Ionic liquids as a novel class of electrolytes in polymeric aqueous biphasic systems. *Process Biochem* **50**:661–668 (2015).
37 Santos JHPM, Martins M, Silvestre AJD, Coutinho JAP and Ventura SPM, Fractionation of phenolic compounds from lignin depolymerisation using polymeric aqueous biphasic systems with ionic surfactants as electrolytes. *Green Chem* **18**:5569–5579 (2016).

38 Merchuk JC, Andrews BA and Asenjo JA, Aqueous two-phase systems for protein separation. *Studies on phase inversion. J Chromatogr B Biomed Sci Appl* **711**:285–293 (1998).
39 Swain AL, Jaskólski M, Housset D, Mohana Rao JK and Wlodawert A, Crystal structure of *Escherichia coli* L-asparaginase, an enzyme used in cancer therapy. *Biochem Commun* **90**:1474–1478 (1993).
40 Dolinsky TJ, Nielsen JE, McCammon JA and Baker NA, PDB2PQR: an automated pipeline for the setup of Poisson-Boltzmann electrostatics calculations. *Nucleic Acids Res* **32**:W665–W667.
41 ExPasy, Amino acid scale: normalized consensus hydrophobicity scale. [Online] (2017). Available: Available from: http://us.expasy.org/tools/pscale/Hphob.Eisenberg.html.
42 Eisenberg D, Schwarz E, Komaromy M and Wall R, Analysis of membrane and surface protein sequences with the hydrophobic moment plot. *J Mol Biol* **179**:125–142 (1984).
43 Hammes W, Schleifer KH and Kandler O, Mode of action of glycine on the biosynthesis of peptidoglycan. *J Bacteriol* **116**:1029–1053 (1973).
44 Sikkema J, de Bont JA and Poolman B, Mechanisms of membrane toxicity of hydrocarbons. *Microbiol Rev* **59**:201–222 (1995).
45 Santos JCF, Moguel IS, Monteiro G, Pessoa-Jr A and Vitolo M, Extracellular secretion improvement of recombinant l-asparaginase II in *Escherichia coli* BL21 (DE3) using glycine and n-dodecane. *Appl Microbiol Biotechnol* 2017.
46 Sanches M, Barbosa JARG, De Oliveira RT, Neto JA and Polikarpov I, Structural comparison of *Escherichia coli* L-asparaginase in two monoclinic space groups. *Acta Crystallogr - Sect D Biol Crystallogr* **59**:416–422 (2003).
47 Sugio S, Kashima A, Mochizuki S, Noda M and Kobayashi K, Crystal structure of human serum albumin at 2.5 A resolution. *Protein Eng* **12**:439–446 (1999).
48 Bujacz A, Structures of bovine, equine and leporine serum albumin. *Acta Crystallogr Sect D Biol Crystallogr* **68**:1278–1289 (2012).
49 Souza RL, Ventura SPM, Soares CMF, Coutinho JAP and Lima ÁS, Lipase purification using ionic liquids as adjuvants in aqueous two-phase systems. *Green Chem* **17**:3026–3034 (2015).
50 Beacham IR, Periplasmic enzymes in gram-negative bacteria. *Int J Biochem* **10**:877–883 (1979).

